JOURNAL OF GEOPHYSICAL RESEARCH, VOL. 95, NO. A9, PAGES 15,059–15,071, SEPTEMBER 1, 1990

Correlation of Whistler Mode Phase Delay With Transient Hydromagnetic Waves

E. W. PASCHAL

STAR Laboratory, Stanford University, Stanford, California

L. J. LANZEROTTI AND C. G. MACLENNAN

AT&T Bell Laboratories, Murray Hill, New Jersey

Changes in the phase delay of a ducted whistler mode signal from the Siple Station VLF transmitter to a receiver at Roberval, Quebec, are compared to variations in the horizontal components of the Earth's magnetic field measured nearby at La Tuque, Quebec. The VLF transmission contains 10.5 min of two distinct tones with 30-Hz separation. Each tone suppresses the cyclotron-resonance growth of the other, eliminating growth-associated phase effects, and allows phase changes due to radial duct motion to be observed. Spectrograms of the VLF phase delay and variations in the components of the geomagnetic field show similar features, with phase features preceding magnetic features by 20 to 30 s. A cross-correlation plot of VLF phase delay and variations in the east-west component shows a bipolar signature which is interpreted as evidence of transient hydromagnetic waves in the 20–45 s band (Pc 3 band) moving from equator to ground. Previous studies have noted correlations between VLF Doppler shifts and resonant hydromagnetic waves, but this is the first report where the VLF phase delay is used directly, and where resolution is sufficient to observe a transient hydromagnetic wave which has a parallel wavelength shorter than the length of the field line.

1. INTRODUCTION

Changes in the phase delay of a VLF whistler mode signal, propagating from a transmitter in one hemisphere through a field-aligned magnetospheric duct to a receiver in the other, are compared with variations in the geomagnetic field observed at the foot of the flux tube. Whistler mode phase delay is largely determined by electron content at the top of the duct near the equatorial plane. The frequencies of observed hydromagnetic waves depend upon the ion content of the plasma and its distribution along a flux tube and, near a wave resonance, are most sensitive to the near-equatorial ion content of the resonating flux tube.

The VLF whistler mode phase delay t_p of a signal on a path S is the time for a given wavefront to propagate from one end of the path to the other, and depends on the refractive index μ along the path. For ducted propagation along a magnetic flux tube through the magnetosphere, the phase delay of a signal at frequency f can be written as

$$t_p = \frac{1}{c}\int_S \mu\, ds \approx \frac{1}{c}\int_S \frac{f_N}{f^{1/2}(f_H - f)^{1/2}}\, ds \qquad (1)$$

where c is the velocity of light, $f_N = 8.98N^{1/2}$ (Hz m$^{3/2}$) is the local plasma frequency, which depends only on the electron number density N, and $f_H = 2.80 \times 10^{10} B$ (Hz T^{-1}) is the electron gyrofrequency, which depends only on the local magnetic field flux density B. Because of the variation of B along S, the total phase delay is determined primarily by conditions near the top of the propagation path where the gyrofrequency is lowest and μ is therefore largest.

Paper number 90JA00206.
0148-0227/90/90JA-00206$05.00

Long-Term Changes

Over times of tens of minutes and longer, the phase delay on a given path may change from several causes [*Thomson*, 1976*a*]. First, azimuthal electric fields in the ionosphere that are mapped up into the magnetosphere will cause $\mathbf{E} \times \mathbf{B}$ drift of the plasma in the duct. An east/west electric field produces an outward/inward duct motion, and a corresponding increasing/decreasing phase delay. (Radial electric fields would cause a duct to drift in longitude; any phase change from such fields would generally be much smaller than in the previous case and would therefore be much harder to measure.) Second, a change in electron density N due to plasma flow into or out of an otherwise stationary duct will affect the phase delay. Other factors remaining constant, an increase in phase delay would occur during the day as solar irradiation heats the upper atmosphere, causing plasma to diffuse into the magnetosphere; the reverse situation would occur at night as plasma moves back down to sustain the ionosphere.

Thomson [1976*b*] used the Doppler shift Δf (proportional to the rate of change of phase delay as $\Delta f = f\, dt_p/dt$) of VLF signals from station NLK to measure electric fields on propagation paths near $L = 2.3$, and obtained field values similar to those found by other methods. *Andrews et al.* [1978] and *Andrews* [1980] used both Doppler shift and change in group delay t_g, which has a different functional dependence on N and B, to separate and measure both the electric field and the plasma flow. Unfortunately, the flow calculation is of only marginal accuracy on individual nights because of errors in determining Δf and t_g, though information on average behavior can be obtained.

Saxton and Smith [1989] extended this work, using signals from two VLF transmitters (NAA and NSS) at different frequencies, which allows the independent determina-

tion of path L value. They calculated a daily plasma flux curve by averaging data over a 9-day period. They used the method of spectrographic group delays described by *Thomson* [1981] to measure Δf and t_g from signals with MSK modulation (the format currently transmitted by U.S. Navy VLF stations). This technique can also distinguish between whistler mode signals propagating in different ducts, like the spectrographic receivers used in previous studies with FSK-modulated signals. However, it requires long integration times, and only one value of Δf and t_g is produced every 15 min. The measurement accuracy is estimated to be ± 0.03 Hz for Δf, and ± 2 ms for t_g.

Short-Term Variations

On the time scale of the magnetic field variations discussed in this paper, geomagnetic fluctuations observed on the ground correspond to hydromagnetic waves in the magnetosphere. These waves can cause changes in VLF phase delay through of changes in duct position (and thus the length of the path of integration S), and to a lesser extent because of changes in B.

Andrews [1977] noted that the phase delay will be affected by meridional motions of the duct near the equator but remain unaffected by azimuthal motions. He studied the correlation between pulsations in the Pc 5 range (having periods from 2.5 to 6 min) and the Doppler shift Δf of whistler mode signals transmitted from NLK (Jim Creek, Washington) at 18.6 kHz as received in Wellington, New Zealand. The whistler mode ducts were at relatively low latitudes ($L = 2.4$–2.6) compared to the Siple-Roberval case discussed here. Whistler mode signals were seen only at night. The Doppler shift of the FSK signals was measured with a spectrographic receiver containing a bank of filters spaced every 0.05 Hz centered at 18.6 kHz. The receiver was designed for long-term studies of duct behavior, and had barely enough time resolution to resolve pulsations with periods as short as 2.5 min. Andrews' experimental data supported the idea that phase path changes are due to radial motion of the duct in the equatorial region. Unfortunately, the time resolution of his measurements was insufficient to observe any delay between VLF phase path changes and magnetic field changes.

Rietveld et al. [1978] reported correlations between whistler mode signals and magnetic pulsations similar to those discussed here. They used signals at 6.6 kHz from a transportable VLF transmitter in Alaska as received in Dunedin, New Zealand ($L = 2.7$). Signals were transmitted in a variety of single-tone formats [*Dowden et al.*, 1978]. The Doppler frequency shift Δf of the signals was measured with the "phasogram" technique during two different events, covering intervals of 14 and 10 min duration. The measurements were correlated with magnetic variations of periods 94 and 60 s, respectively. The whistler mode signals in these two events were determined to have travelled in ducts at $L = 3.77$ and 2.85, respectively. The magnetic pulsations were measured in Dunedin with a horizontal loop as dZ/dt, where Z is the vertical magnetic field component. *Rietveld et al.* [1978] plotted the cross-correlations of Doppler shift Δf and dZ/dt versus lag time for their two events. For the first event, they found a time delay of 24 s, with Δf lagging dZ/dt (correlation $\rho = 0.4$), approximately one-quarter of the 94 s period of the pulsation. For the second event, they found a time delay of 10 s, again with Δf lagging dZ/dt ($\rho = 0.95$), somewhat less than the quarter-period of the 60 s pulsation. They concluded that Δf and dZ/dt were in phase quadrature. They interpreted this as being consistent with VLF signal modulation by the lowest-order resonant oscillation of a field line; that is, a standing wave with an antinode (and maximum radial motion) near the equator.

In this paper we present a new technique for making phase path measurements using a two-tone signal from the Siple VLF transmitter combined with signal phase analysis. We compare the measurements from one such transmission with geomagnetic data taken at the same time, and interpret the results in terms of transient hydromagnetic waves travelling down the field line. Finally, we discuss the advantages and limitations of this technique in comparison to those used in the studies mentioned above.

2. SIGNALS SUITABLE FOR PHASE MEASUREMENT

The VLF transmitter at Siple Station, Antarctica (local time $\approx$ UT -5 hours), is a controlled source of whistler mode signals on paths near $L = 4$, and can be used for monitoring VLF propagation path phase delays. The obvious approach would be to transmit a constant-frequency signal from Siple and measure its relative phase (i.e., phase with respect to a reference oscillator at the transmitted frequency) at the conjugate end of the path near Roberval, Quebec. Unfortunately, unlike the NLK signals propagating near $L = 2.3$ (see above), a single-frequency signal from Siple is very likely to show amplitude growth caused by wave-particle interactions. The phase advance associated with this growth will completely mask any smaller phase changes due to duct motion [*Paschal and Helliwell*, 1984]. The maximum observed rate of phase change of Siple signals associated with duct motion is less than ± 1 rev $s^{-1} = \pm 1$ Hz. (One revolution, or rev, equals 2π radians. An advance of one rev in the relative phase of a signal at frequency f is caused by a one-wavelength decrease in the path phase length, or equivalently a decrease of $1/f$ seconds in the phase delay t_p. A relative phase advance at a rate of 1 rev s^{-1} gives a Doppler shift of $+1$ Hz.) In contrast, cyclotron-resonance growth may produce frequency offsets of as much as 10 Hz (with phase advances up to 2 revs) prior to triggering emissions, and 100 Hz or more if triggered emissions occur [*Paschal*, 1988]. However, if two signals separated in frequency by about 20 to 30 Hz are transmitted, then each signal will tend to suppress the growth of the other [*Chang et al.*, 1980]. The result in this case can be a stable signal without growth-related phase advances, suitable for phase delay studies. Other effects of wave-particle interactions, such as the generation of coherent sidebands, may be seen, but these effects will not alter the phases of the two transmitted components.

The Two-Tone LICO1 Format

The spectrogram in the top half of Figure 1 shows the start of a LICO1 (line coupling, version 1) transmission from the Siple transmitter as received at Roberval. The LICO1 format contained 10.5 min of a two-tone transmission with components at 3950 and 3980 Hz (i.e., 30 Hz separation), followed by some 2.5 min of LICO-type format (10-s segments of single tones and tone-pairs with various separations). The important data section is thus the first

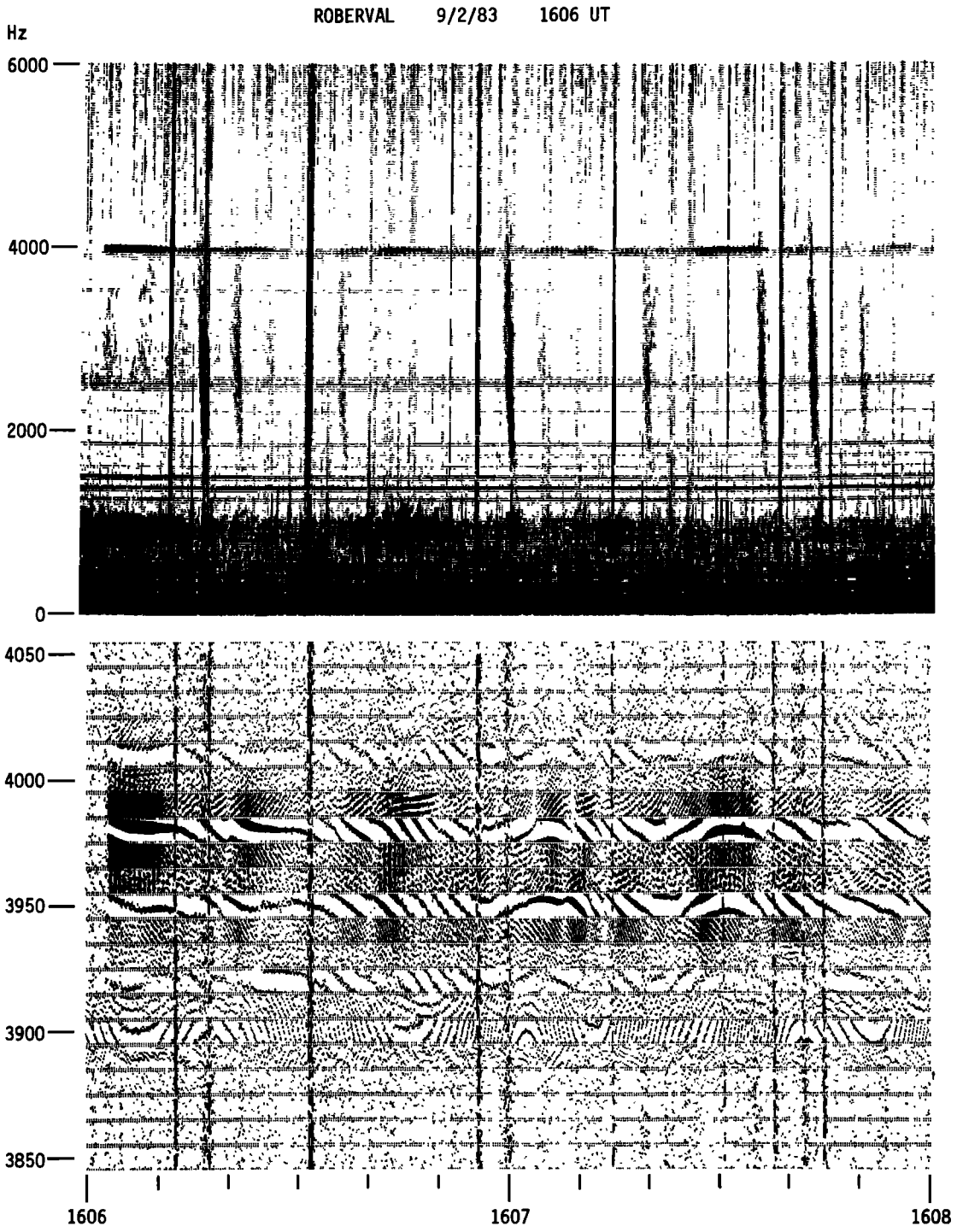

Fig. 1. Spectrogram and phase plot of a two-tone LICO1 transmission from Siple Station as received at Roberval. The phase plot shows the outputs of 20-Hz-wide analysis filters spaced every 10 Hz, with trace width proportional to filtered signal magnitude and trace position to relative phase (1 rev full scale). The LICO1 tones at 3950 and 3980 Hz begin at 1606:03 UT. The transmitted tones show phase changes due to motion of the magnetospheric path. Also present are sidebands at 3920 and 4010 Hz, and local power-line interference near 3900 and 4020 Hz.

10.5 min of the LICO1 format. The two-tone signal started at 1606:03.1 UT (after a group delay of t_g = 2.1 s) and continued for 10 min 29 s until the LICO format began at 1616:32.1 UT. The two-tone signal faded in and out with an approximately 10 to 30-s period, but it was always visible. Though the signal was strong, it did not show any spectral broadening or any triggered emissions, characteristics associated with particle-induced growth and phase instability. (The spectrogram in Figure 1 also shows a weak 1.5-Hz modulation; this is an artifact of the analysis due to aliasing of the 30 Hz beat in the signal by the output plotting step time t_{step} = 0.1906 s.)

There were frequent whistlers, somewhat compressed in Figure 1, with one-hop delay times ranging from 2.1 s up-

wards. (There were also a few weak components with delays from 2.0 to 2.1 s.) The whistler nose frequencies (frequencies of minimum group delay) were near 3.5 to 4 kHz. Some of these whistlers were seen to generate precursors on the LICO1 signal, but these caused only momentary perturbations. (Precursors are discrete emissions or enhancements in wave growth associated with whistlers but which precede the two-hop whistler echo; see *Paschal* [1990] for details of these particular events.) Since their group delays were the same, it is reasonable to assume that the Siple signal was propagating on the same path as the first strong component of the nose whistlers. The standard methods of whistler analysis can then be used to find the magnetospheric path latitude and flux tube electron density. Using a nose frequency of $f_n = 4000$ Hz and a nose group delay of $t_n = 2.1$ s, we find from *Park* [1972] a path L value of $L = 4.32$ and a hemispheric tube content (the total electron density per unit area of flux tube at 1000 km, integrated from the ionosphere to the equatorial plane) of $N_T = 3.5 \times 10^{13}$ cm^{-2}. This corresponds to an equatorial electron density of $N_{eq} = 275$ cm^{-3}, a typical value for the outer regions of the plasmasphere under magnetically quiet conditions [*Park et al.*, 1978].

The gray-scale phase plot in the bottom half of Figure 1 shows the phase behavior at the beginning of the LICO1 signal. Timing errors due to wow and flutter in the analog field recording have been corrected, and signal phases reconstructed, by tracking a recorded constant-frequency pilot tone as described by *Paschal and Helliwell* [1984]. Each horizontal band in the figure shows the output of one analysis filter (spaced every 10 Hz, the bandwidth of each filter is 20 Hz). The filtered signal trace width is proportional to signal magnitude; and the trace deflection is proportional to relative signal phase (phase with respect to the center frequency of the filter), 1 rev corresponding to full scale. Signal leakage (together with sampling during plotting) causes the striped effects seen in filters adjacent to strong components (e.g., in the filters at 3960, 3970, and 3990 Hz).

Both the 3950 and 3980 Hz components in the filtered signal, corresponding to the transmitted frequencies, showed slow phase changes characteristic of duct motion. The maximum Doppler frequency offset in Figure 1 occurs at 1606:50 UT, when both components show a −0.3 Hz shift (i.e., a decrease in relative phase of 3 revs in 10 s). Doppler shifts at other times reached as much as ±0.5 Hz. Both transmitted components showed similar, though not identical, phase behavior. Each signal showed periods of fading, sometimes with 1/2-rev jumps in phase. A good example is at 1607:37 UT on the 3980-Hz component. The fading and phase jumps were probably caused by beating between transmitted signals which were propagating in different but nearby ducts. This interference must be due to differential changes in path length in the magnetosphere since that part of the path, with a phase delay of $t_p = 3.23$ s (see section 3). is almost 13,000 wavelengths long at 3980 Hz, while the total subionospheric path, say 300 km, is only four wavelengths long. Note that the amplitude nulls and phase jumps in Figure 1 occur at different times in the signals at the two frequencies. There is also a small blip in the phase of the 3980-Hz tone (an increase of 1/4 rev) due to a whistler precursor at 1607:34 UT, but its effect lasts for less than a second.

Weak sidebands at 30 Hz below and above the transmitted signals (at 3920 and 4010 Hz) were present through most of the 10 min 29 s two-tone transmission. Weaker sidebands at 60 Hz below and above the transmitted frequencies (3890 and 4040 Hz) were also seen occasionally, although they are not evident in the data segment shown in Figure 1. The phases of the sidebands tracked those of the main signals. The existence of sidebands indicates that some nonlinear process is occurring, and is evidence of wave-particle interactions.

There were also signals at 3900 and 4020 Hz. These were power-line signals at the 65th and 67th harmonics of 60 Hz picked up locally at the receiver, and do not interfere with the analysis. As expected, the phase variations of these power-line harmonics had no correlation with the Siple signal phases.

Evidence Against Particle-Induced Phase Effects

We must be sure that the phase changes evident in Figure 1 were due only to changes in the effective length of the path of propagation and were not corrupted by spurious effects due to wave-particle interactions. The most common evidence of wave-particle interactions is the growth in amplitude of an input signal accompanied by a simultaneous advance in relative phase. Growth and phase advance almost invariably occur together [*Paschal and Helliwell*, 1984; *Paschal*, 1988]. (Amplitude decline may also be associated with phase retardation, but the published evidence here is not as extensive. Examples of this type are rare because signals amplified by wave-particle interactions tend to terminate by generating emissions rather than by slowly dying away.)

There is no correlation evident in Figure 1 between amplitude and phase that might indicate growth-related phase effects. Such a noncorrelation held throughout the approximately 10-min interval. Changes in wave amplitude appeared to have occurred independently of changes in phase (except for the rapid phase changes accompanying fading that always occurred at amplitude nulls). Amplitude growth is seen to occur both when the relative phase is retarding, as at 1606:20 and 1606:40 UT, as well as when the relative phase is advancing, as at 1607:25 UT. Since those overall changes in phase that occurred simultaneously on both transmitted signal components appear to be unrelated to signal amplitude, they are therefore likely to be due only to changes in the path of propagation.

However, we note that the phase variations of the two input signal components were not identical. While the common large-scale phase changes are probably not caused by particle effects, the possibility remains that the differences in phase behavior of the two frequencies were still due to wave-particle interactions. To test this possibility, the data were analyzed by plotting the amplitude and phase of the 3950-Hz component while tracking on the 3980-Hz signal instead of the pilot tone (plot not shown). Tracking on the higher-frequency signal removes those phase variations common to both components so the plot at 3950 Hz would show only the differential phase behavior. If there were any residual particle-induced phase effects, it might be expected that this differential phase would be correlated with the difference in signal amplitudes. In fact, it was found that the transmitted signals faded slowly, with a period of 5 s or more, often independently on each frequency, sometimes with deep nulls. The differential phase (i.e., $\phi_{3950} - \phi_{3980}$) showed changes

of about 1 rev, sometimes correlated with the difference in amplitudes at the two transmitted frequencies (consistent with a phase advance caused by the growth of one signal with respect to the other), but just as often not correlated or even anticorrelated. We conclude that the differential phase changes were not due to differential growth but most likely were just the result of multipath interference in the magnetosphere.

Removing Fading and Other Artifacts

The next step in the analysis extracted the phase information from the LICO1 signal and put it in a form suitable for further processing. Two analysis filters were used to separate the two transmitted components at 3950 and 3980 Hz. One output point was calculated for each filter every 250 ms. Phase was measured relative to the center frequency of each filter; that is, the inherent phase advance of 3950 or 3980 rev s^{-1} at the filter output was subtracted. Figure 2 shows the relative phases of the filtered LICO1 components, plotted modulo 20 revs, as a function of time from 1606 to 1617 UT. Phase decreased from the initially defined value of 0 in both cases to around −100 revs at 3950 Hz and about −90 revs at 3980 Hz by the end of the two-tone transmission.

The ϕ_{3950} and ϕ_{3980} plots in Figure 2 contain artifacts of several kinds. Those marked "F" were due to fading; these sometimes included a 1/2-rev jump in phase while at other times there was just a momentary change. Fading jumps occurred as the amplitude of a signal component went through a null, and happened at different times for the two frequencies. Fading due to differential changes in the phase delays of multipath signals can be likened to beating between two signals at close but not identical frequencies. Given two equal-amplitude signals, $\cos\omega_a t$ and $\cos\omega_b t$, their sum can be expressed as $2\cos\frac{1}{2}(\omega_b-\omega_a)t\cos\frac{1}{2}(\omega_a+\omega_b)t$; that is, a carrier at the average frequency $(\omega_a+\omega_b)/2$ modulated by the function $\cos\frac{1}{2}(\omega_b-\omega_a)t$ at half the difference frequency. Note that the modulating function alternates in sign with each beat, so the relative phase of the carrier changes by 1/2 rev at each null in amplitude. In the case of real fading, the two (or more) signals involved are unlikely to have exactly equal amplitudes, so there may not be a precise null in amplitude between beats. Whether the change in phase from one beat to the next will be observed as +1/2 rev or −1/2 rev depends on which signal is stronger at the time.

Because the magnetospheric path is so long, phase jumps due to fading would not be expected to occur at the same time at 3950 Hz as at 3980 Hz, nor necessarily to be of the same sign. Different fading behavior at the two frequencies can cause cumulative differences in the phases of the two signals. An example of this is seen in Figure 2 around 1608 UT, where the phase at 3980 Hz shows a slower average decrease than that at 3950 Hz. In addition to any cumulative errors, fading certainly increases the short-term noise of the phase traces.

Figure 2 also shows the combined phase ϕ_c (labeled "Weighted Sum") derived from the two filter outputs by summing the incremental phase advance at each frequency weighted by the instantaneous amplitude of that component. That is, at time $t = 250n$ ms, the combined phase $\phi_c(n)$ is calculated from its value at the previous sampling interval together with the phases and amplitudes of the filtered signal components as

$$\phi_c(n) = \phi_c(n-1) + \frac{A_{3950}(n)\delta\phi_{3950}(n) + A_{3980}(n)\delta\phi_{3980}(n)}{A_{3950}(n) + A_{3980}(n)} \quad (2)$$

where $A_{3950}(n)$ is the current amplitude, and $\delta\phi_{3950}(n) = \phi_{3950}(n) - \phi_{3950}(n-1)$ is the change in phase from the previous sample of the filtered component at 3950 Hz; and similarly at 3980 Hz. Note that if the amplitudes of the two filtered components were always equal, the combined phase would just be the average of ϕ_{3950} and ϕ_{3980}. However, when their amplitudes differ, the combined phase tends to follow the phase behavior of the stronger component. The utility of the combined phase ϕ_c is as follows: when a phase jump due to fading occurs in one filtered component, it occurs near an amplitude null for that component, at which time the other component is generally not experiencing a phase jump or amplitude null; the combined phase, following the stronger component, tends not to show the effects of fading. The combined phase ϕ_c therefore gives a clearer, less noisy picture of actual changes occurring in the magnetosphere. For practical purposes, ϕ_c can be regarded as the relative phase of a single-frequency signal, at a mean frequency of 3965 Hz, which has propagated on a single whistler mode path without distortion by wave-particle interactions or fading.

The features marked "S" and "W" were phase jumps due to spherics and whistlers or whistler precursors. To the extent that these were more detrimental to weaker signals, their effects were also reduced by the combined phase procedure. The effect of one spheric, at 1611:44.5 UT, was removed by hand from ϕ_c by forcing the phase to remain constant for one sample (250 ms) at that time. Two pilot-tone tracker errors, labeled "T" at 1613 16.5 and 1615:46.5 UT, were similarly explicitly removed.

The features marked "WWV" were 8-s breaks in the data during which the audio timing signal from a shortwave receiver was recorded. There was no LICO1 signal on the tape during these intervals and the phase behavior observed is spurious. There was also a mysterious 20-s interval of missing data labeled "break." The cause of this omission is unknown, but it might have been due to an equipment malfunction or an operator error that momentarily stopped the field tape recorder. Both WWV breaks and the missing data interval were removed from ϕ_c by holding the phase constant for the appropriate time. This is a simple way to fill in missing data, of course, but it might also introduce artifacts. The reader may judge whether a straight line of some different slope, or perhaps a spline curve, might have better bridged the gaps.

Finally, the two features near the end marked "E" were emissions from the first two single-tone segments of the following LICO transmission format. The 10-s segment between them was a two-tone LICO segment, also at 3950/3980 Hz, and we desired to include it with the preceding data. We ignored the first set of emissions since they didn't seem too noisy, and terminated ϕ_c at the start of the second set. The total sequence of phase samples ϕ_c thus runs from 1606:03 through 1616:52.5 UT.

3. MAGNETIC FIELD AND PHASE DATA COMPARED

Plotted in the top two traces of Figure 3 are the magnetic south-north (H) and west-east (D) components of the

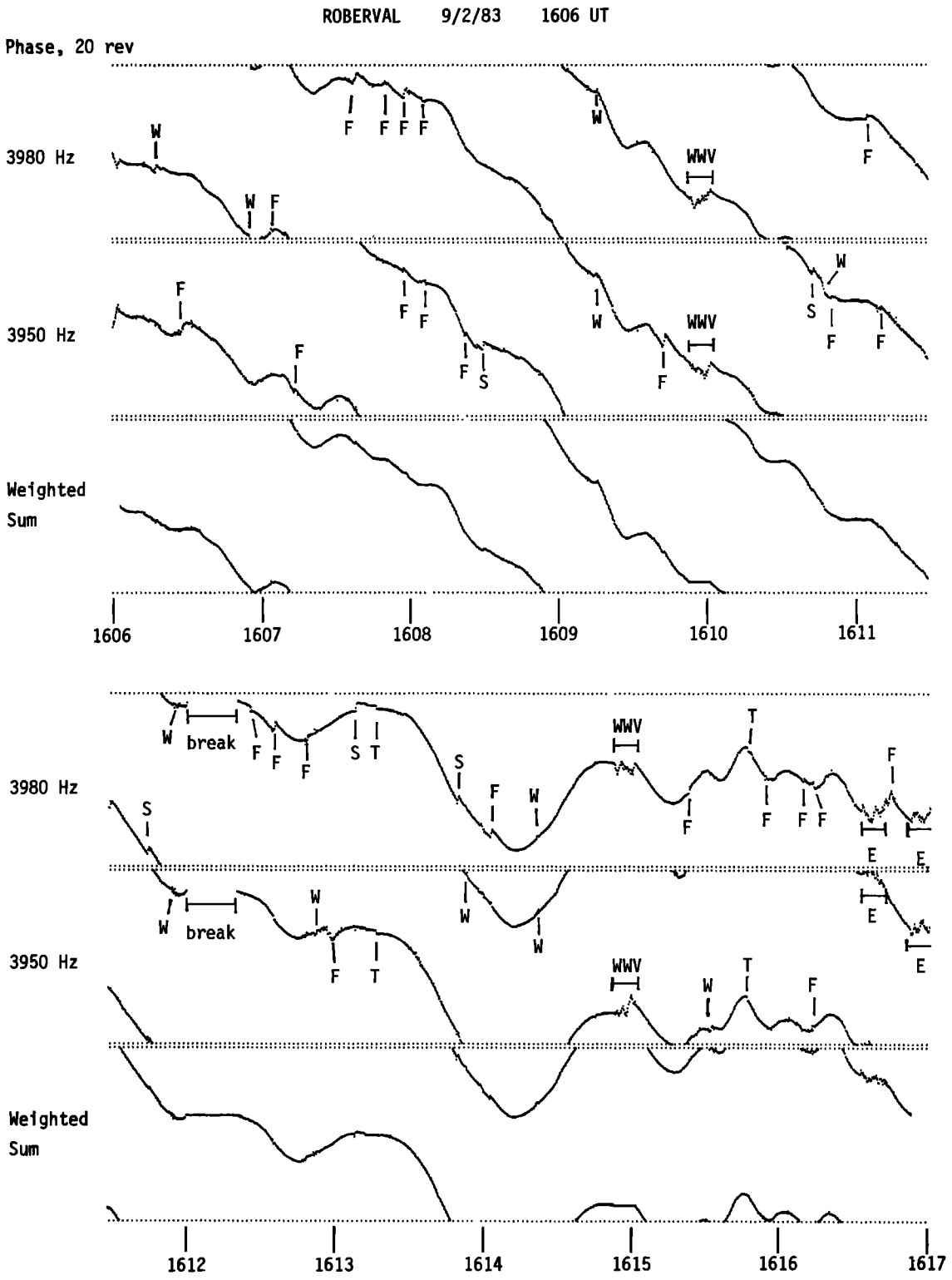

Fig. 2. Phase of the received LICO1 signal. The plots at 3980 and 3950 Hz are the actual signal components (filter BW = 16 Hz, 20 rev full scale). The plot "Weighted Sum" is the combined phase ϕ_c corrected for fading, data breaks, and tracking errors. Data features: *E*, emissions; *F*, fading; *S*, spheric; *T*, pilot tracker error; *W*, whistler and/or whistler precursor; *WWV*, time signal break; break, 20-s break in data.

Earth's magnetic field as measured by the Bell Laboratories magnetometer at La Tuque, Quebec, 87 km south-southwest of Roberval, at $L \approx 3.9$ [*Stassinopoulos et al.*, 1984]. The third trace shows the LICO1 combined phase ϕ_c from Figure 2. The noise level in each magnetic component was ≈ 0.2 nT. The magnetic field was sampled at 2-s intervals with digitization increments of 0.06 nT.

Since the phase delay ϕ_c values were determined each 250 ms, values of the magnetic field components were generated at quarter-second intervals by interpolation to match

the phase data. This was done by assuming that each magnetic field component was constant during the 2-s interval centered on the actual sample. The absolute timing error in the magnetometer data was less than 1 s. Timing errors in the VLF phase data are at most a few milliseconds and can be ignored.

There are two different types of behavior evident in Figure 3: slow drifting with a scale time of many minutes, and smaller ripples with periods in the range of 20 to 40 s. All three signals showed somewhat similar long-term behavior. The magnetic field changed slowly, H increasing and D decreasing, over a range of about 10 nT, and the VLF phase decreased (phase path became longer) by about 100 rev (25.2 ms), until 1614 UT. At that time, H reversed its behavior and started to decrease, and D and ϕ_c stopped decreasing and remained more or less constant.

Long-term changes in magnetic field strength and VLF phase may not be related. Some mechanisms can cause a change in phase path length without any corresponding change in the Earth's magnetic field. For instance, the drift in phase delay might represent $\mathbf{E} \times \mathbf{B}$ drift of the duct due to magnetospheric electric fields, a situation which would not imply any corresponding change in magnetic field.

On the other hand, for the data set studied here, the local time at both ends of the magnetospheric path was shortly before noon, and both ionospheres were in sunlight (solar elevation only 5° at Siple). The longer-term increase in phase delay (decrease in ϕ_c) might merely reflect increasing plasma density in the magnetosphere due to diffusion up from the sunlit ionospheres, again a situation not connected with magnetic field changes. From *Paschal* [1988, Appendix B] we find that a signal on a path at $L = 4.32$, at a frequency of 3965 Hz and with a group delay of $t_g = 2.1$ s, will have a total phase delay of $t_p = 3.23$ s. As noted above, the tube content is $N_T = 3.5 \times 10^{13}$ cm^{-2}. A plasma flux dN_T/dt will cause a change in phase delay of $dt_p/dt = (t_p/2N_T)\, dN_T/dt$ [*Andrews et al.*, 1978]. Using an upward flux of $dN_T/dt = 3 \times 10^8$ cm^{-2}s^{-1} (*Park*'s [1970] typical value) we find a Doppler shift of −0.055 Hz. That is, upward flux due to solar irradiation might have accounted for one-third of the total −100 revs/11 min = −0.152 Hz average shift in Figure 3.

The faster variations seen in the three traces of Figure 3 have periods in the range of 20 to 40 s. The magnetic variations have peak values of one or two nT. Magnetic variations of this frequency are classified as Pc 3 pulsations. Over the period of a pulsation, the plasma flow between the ionosphere and the magnetosphere would be negligible, so phase variations on this time scale could not be due to changes in tube content.

However, as noted above, changes in phase delay will occur due to changes in duct length S (and to a lesser extent B) caused by the hydromagnetic waves. An inward displacement of a duct would produce a decrease in phase delay; that is, an increase in relative phase ϕ.

All three data sets were high-pass filtered in order to eliminate the large, long-term variations that obscure the pulsation activity. The filter used was simple: a block average in a 32-s interval centered at each sample point was subtracted from that sample. With this filter, components with periods of 10 min or longer are attenuated by 46 dB or more whereas components with periods of 40 s or less are attenuated by

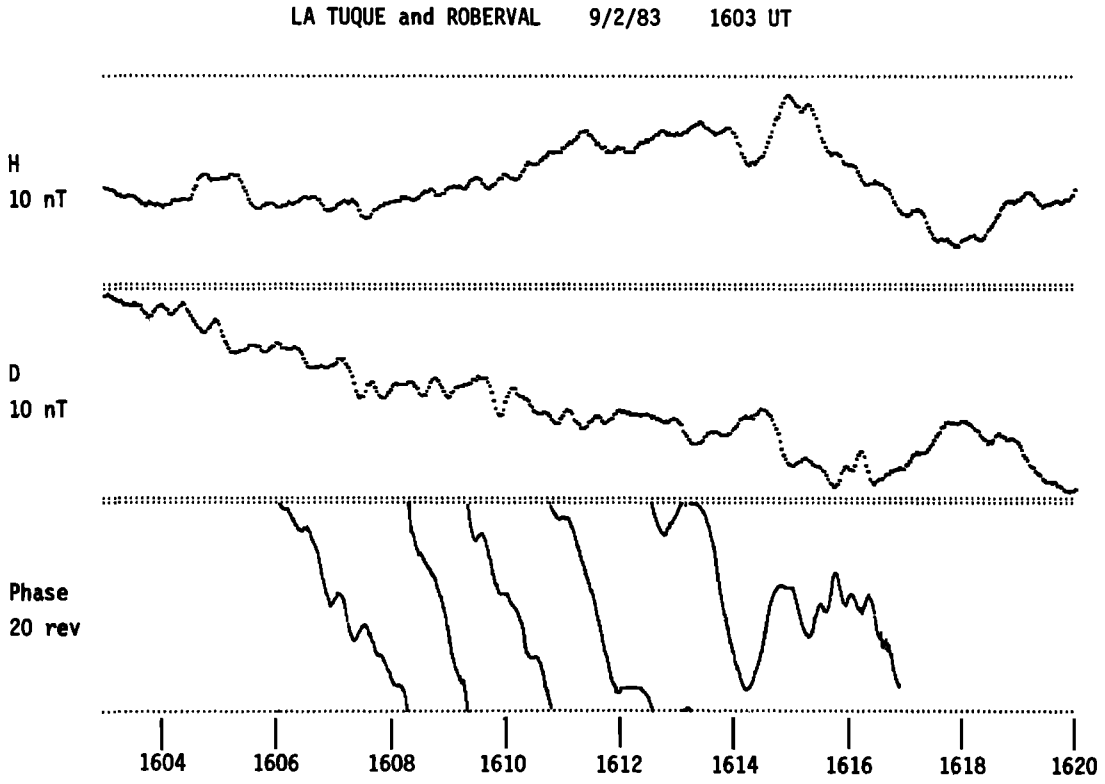

Fig. 3. La Tuque magnetometer components H and D (10 nT = 10γ full scale), and Roberval VLF phase ϕ_c (20 rev full scale). All three signals show small fluctuations with periods of 20–40 s on top of larger changes occurring over many minutes.

at most 2 dB. (The filter has about 3 dB of passband ripple, not very important in this particular case.)

Figure 4 shows the filtered H, D, and ϕ_c signals. The long-period variations have been eliminated, leaving only the Pc 3 pulsations. The signals look fairly complicated, and probably contain energy over at least an octave in frequency. The rms values of the signals (from 1606:19 to 1616:36.5 UT) are $H = 0.200$ nT, $D = 0.282$ nT, and $\phi_c = 0.837$ rev (211 μs). Note that the phase signal has shrunk by 16 s at each end from 1606:03–1616:52.5 UT in Figure 3 to 1606:19–1616:36.5 UT; this is due to the filter procedure.

In order to better visualize the structure of the filtered signals, *f-t* spectrograms were made, as shown in Figure 5. The FFT algorithm was used on 512-sample (128 s) blocks of data. The data window was advanced by $t_{step} = 8$ s to generate each new raster in the plot. With the weighting function used (the 4th-order minimum-sidelobe window of *Nuttall* [1981]), the correlation between transformed blocks drops to less than 50% after an advance of only 32 s, which is thus the effective time resolution of the spectrogram. Analysis filters are spaced every 0.001 Hz, though the bandwidth of each filter is about 0.015 Hz. (See *Paschal* [1988] for the synthesis of closely-spaced filters by interpolation in the DFT spectrum.)

All three spectrograms show similar features. The features extending below 0.02 Hz down to zero frequency from 1614 to 1616 UT are remnants of the long-period variations that have not been completely filtered out. These features are strongest in the H and phase plots, though also slightly present in the D plot. As mentioned above, there may or may not necessarily be a connection between magnetic field and path length behavior at these lowest frequencies, though there does seem to be some similarity here.

More interesting are the Pc 3 signals above 0.025 Hz (period ≤ 40 s). There are strong similarities between features in the first half of the phase plot and corresponding features in D and, to a lesser extent, H. In particular, note that the phase features seem to precede those in D by 20 to 30 s. (This is most easily seen by tilting the page and viewing it from the bottom. Successive rasters in the plot are spaced by $t_{step} = 8$ s.) There is a similar correlation between phase and H, though it is not as strong.

Figure 6 shows plots of the cross-correlation among the three filtered signals as a function of lag time. The cross-correlations were made by using the full length of the sequence of phase samples ($N = 2471$) and lagging them over the longer sequences of H and D. To facilitate comparison, the H versus D plot was made using 2471 samples of D covering the same time interval as ϕ_c, even though more magnetometer data were available.

Figure 6 shows rather little correlation between H and D. This was confirmed by investigating hodograms of H versus D (of both unfiltered and filtered data), which showed no preferential polarizations. There is some correlation (0.43) between H and ϕ_c, with VLF phase preceding magnetic field by 18 s. There is a stronger correlation (-0.55) between D and ϕ_c, again with VLF phase leading by 18 s. (The negative sign in -0.55, of course, means that an increase in ϕ_c is correlated with a decrease in D, or ϕ_c is correlated with $-D$.) There is also a correlation, almost as large in the opposite sense (0.52), between $+D$ and ϕ_c, with VLF phase leading by 30 s. Thus, the correlation plots quantify the

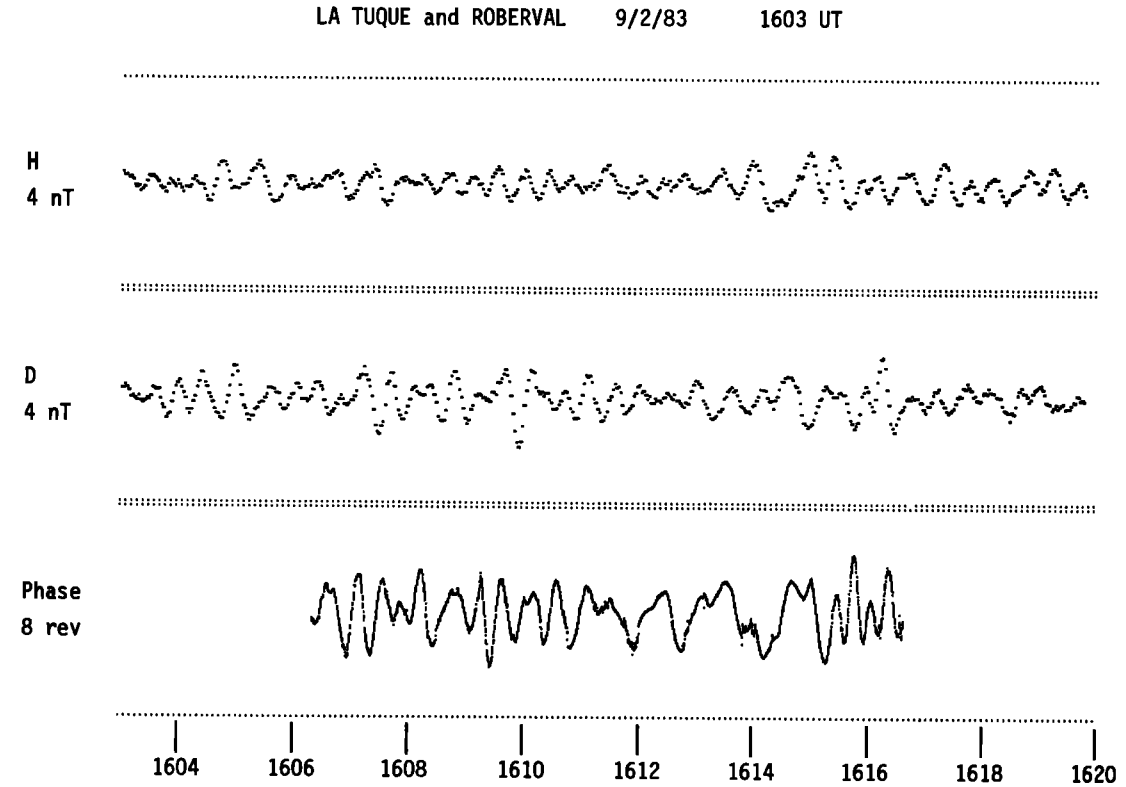

Fig. 4. La Tuque magnetometer components H and D, and Roberval VLF phase ϕ_c from Figure 3, high-pass filtered by subtracting a running average with a 32-s time constant. Note the change in scale to 4 nT/8 rev full scale. The long-period variations have been filtered out and the Pc 3 pulsations are more obvious.

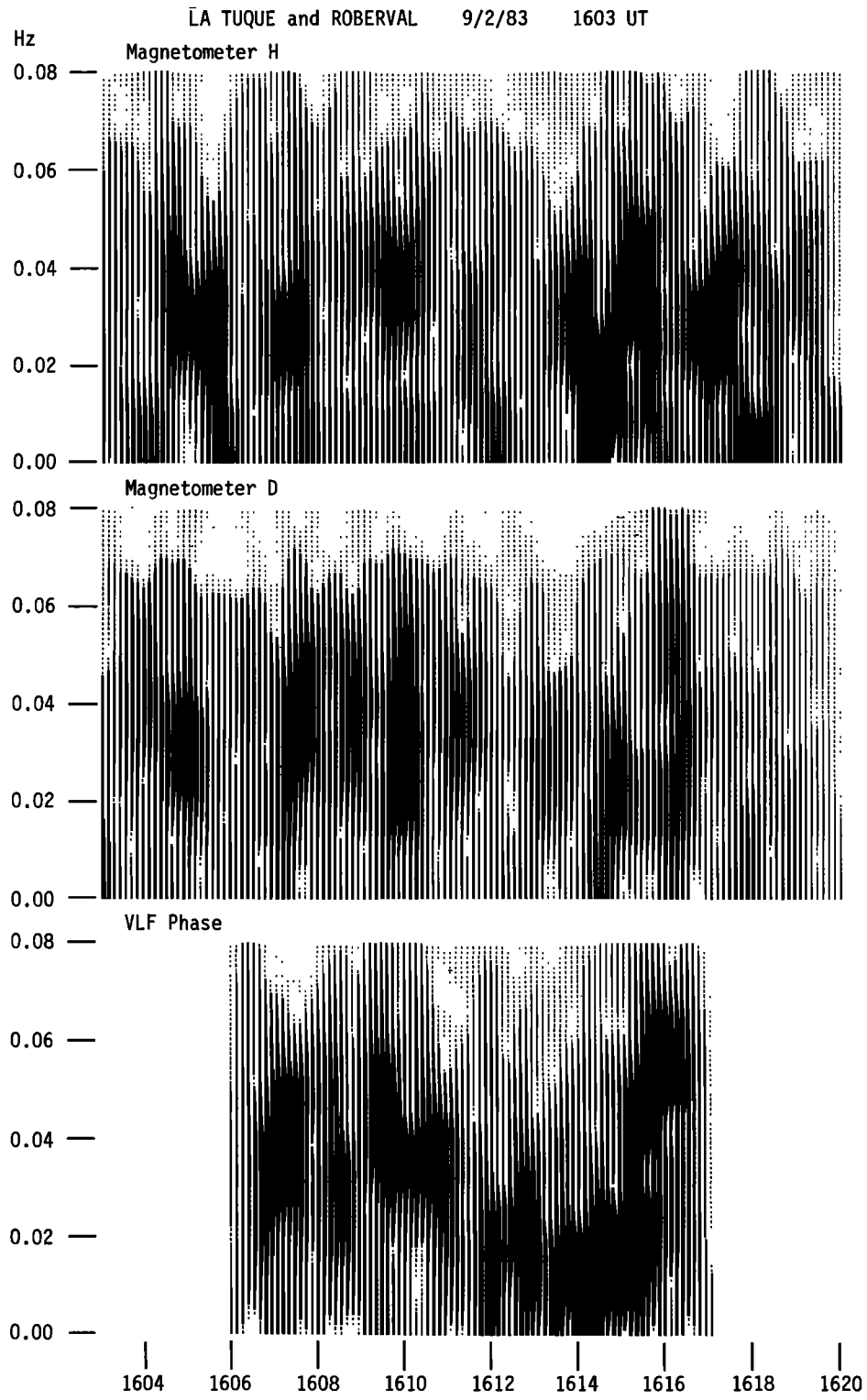

Fig. 5. Spectrograms of the filtered magnetometer and VLF phase data in Figure 4. Similar features can be seen in all three plots. In particular, VLF phase features from 0.025 to 0.05 Hz at 1606–1612 UT seem to precede similar features in D by 20 to 30 s.

correlation and time relations between the VLF phase and the magnetic field variations which are visually very evident in Figure 5.

4. Discussion

The spectrograms of the high-pass filtered data in Figure 5 show similar spectral features in both the magnetic pulsation signals and the VLF phase data. The cross-correlation plots in Figure 6 show that phase changes preceded magnetic field changes by 18–30 s. The VLF phase is most sensitive to conditions (electron density and magnetic field strength) at the top of the whistler mode path where the wave spends most of its time. The magnetometer, of course, measures conditions at ground level at one

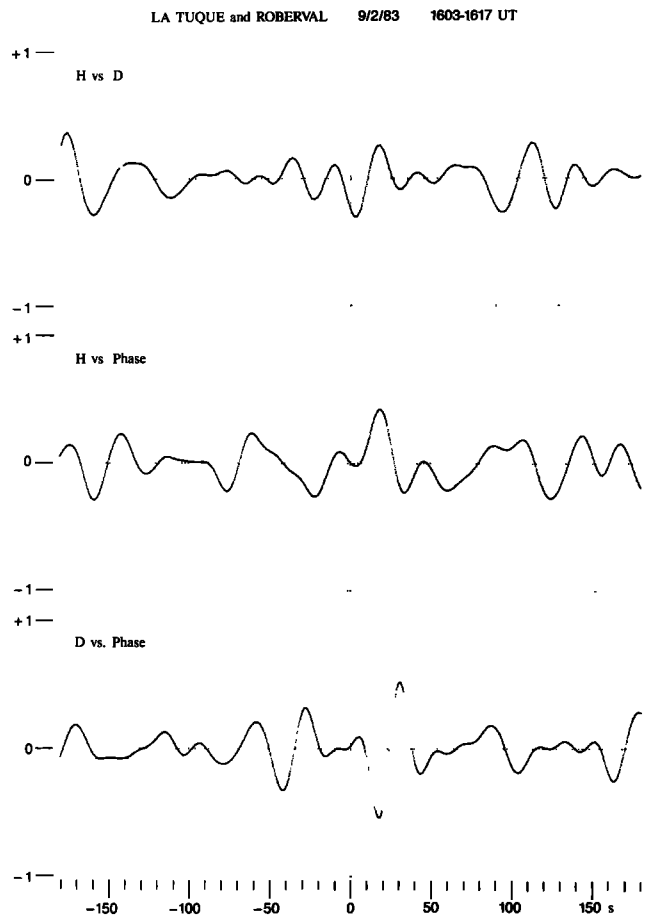

Fig. 6. Cross-correlation plots of the filtered magnetometer and VLF phase data in Figure 4. In each plot, the second variable lags the first for negative offset times, and leads it for positive times. There is little correlation between H and D. Both H and D show some correlation with VLF phase. The correlation between D and VLF phase is bipolar, −0.55 with phase leading magnetic field by 18 s and +0.52 with phase leading by 30 s.

end of the path. At the time of the events studied here the magnetospheric flux tube was on the dayside of the Earth, approaching local noon.

It is most interesting to find that the highest correlation between the VLF phase occurs with the magnetic fluctuations in the east-west component signal. This is readily understood in the context of the discussions of *Hughes and Southwood* [1976] and *Inoue* [1973]. These works show that the ionosphere causes a $\pi/2$ rotation (in a left-handed sense with respect to the Earth's magnetic field) in the orientation of a magnetospheric hydromagnetic wave signal whose magnetic signature is detected on the ground (see also review by *Hasegawa and Lanzerotti* [1978]). There is also other experimental evidence for this effect [*e.g., Andrews et al.*, 1979]. Hence, the east-west (D component) wave signal on the ground is actually the north-south wave signal above the ionosphere. Mapped to the equatorial regions, this signal produces meridional displacements of the magnetic field, the direction of which is expected to produce the largest VLF phase variations [*Andrews*, 1977].

The VLF phase delay is primarily sensitive to HM-wave induced displacements near the equator, as opposed to displacements further down the field line, for a number of reasons. First, the refractive index μ in equation (1) is highest at the top of the path. Calculations using the DE 1 plasmasphere model of *Park* [1972] (containing 90% O^+, 8% He^+, and 2% H^+ at 1000-km altitude in diffusive equilibrium at a temperature of 1600 K), for the path parameters observed here ($L = 4.32$, $N_{eq} = 275$ cm^{-3}), show that the refractive index for a 3965-Hz ducted whistler mode wave is $\mu = 28.6$ at the equator (field-line distance from the surface $s = 31,461$ km), and only $\mu = 5.3$ at a latitude of 57° ($s = 1831$ km). Over 50% of the phase delay (and almost 60% of the group delay) is accumulated within 20° latitude (10,000 km) of the equator.

Second, the change in path length S for meridional displacement at a given latitude depends on the curvature K (the inverse of the radius of curvature) of the field line at that latitude. The curvature at the equator is $K = 1.09 \times 10^{-4}$ km^{-1} compared to $K = 0.62 \times 10^{-4}$ km^{-1} at $s = 1831$ km. The product μK, or the sensitivity of the phase delay to meridional displacement, is thus over nine times greater at the equator than at latitude 57° near the bottom of the field line.

(Accompanying the meridional displacement due to a hydromagnetic wave there may also be a change in local geomagnetic field strength B. However, for VLF frequencies well below the gyrofrequency f_H, the refractive index μ in equation (1) is approximately $f_N/(ff_H)^{1/2}$, which for a given signal frequency f is proportional to the ratio $(N/B)^{1/2}$. This approximation becomes increasingly accurate at lower altitudes as f_H increases. Note that the ratio N/B of plasma density to field strength is unchanged by a transverse HM wave in a homogeneous magnetic field. To the extent it remains constant during a magnetic pulsation in the Earth's field, any changes in phase delay are due to changes in the length of the path of integration S rather than changes in B.)

Finally, the displacement caused by a given hydromagnetic wave will tend to diminish as the wave travels down a field line because of the increase in geomagnetic flux density B. (There are some HM wave solutions, such as even-order standing wave field-line resonances with a displacement null at the equator, for which this is not true. However, the case discussed here is not thought to be one of these exceptions.) So, the effect of a given hydromagnetic wave on the VLF phase delay can be expected to occur almost entirely in the equatorial region of the flux tube.

The features seen in the spectrograms in Figure 5 were short-lived pulsations. At a frequency of 0.04 Hz, the period of the pulsations was about 25 s. However, each feature lasted for only a few cycles at most. These were thus a series of individual transient pulsations. The delay between the VLF phase features and the magnetic features means that these transients occurred first near the equatorial region (where they affected the VLF signal) and only later were observed on the ground (as changes in the magnetic field components)

Interpretation of This Event

The spectral features can be interpreted in terms of the model in Figure 7. A hydromagnetic wave produces a meridional displacement of the equatorial region of the Siple-Roberval field line. This affects the phase of the LICO1 VLF signal from Siple, which takes half of the one-hop whistler

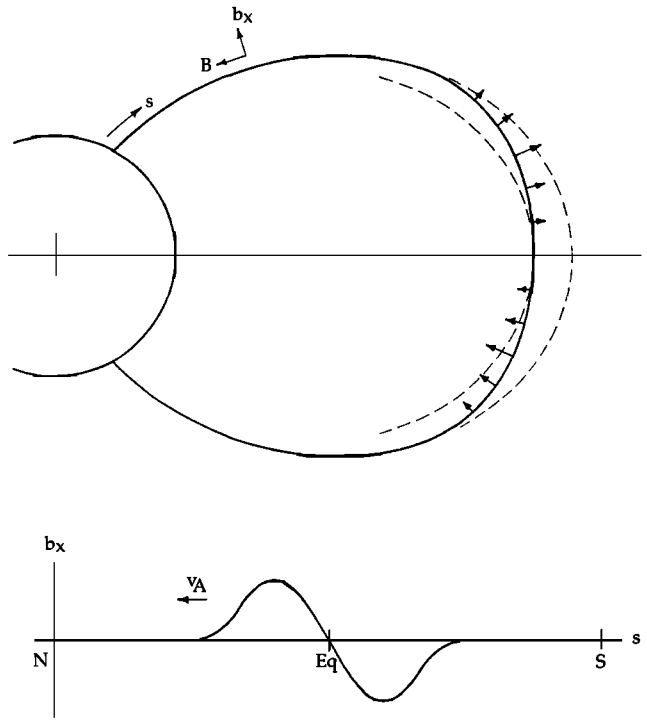

Fig. 7. Field line model showing duct displacement and associated meridional magnetic field b_x due to a transient hydromagnetic wave. Maximum change in VLF phase delay occurs when the wave is at the top of the path. The hydromagnetic wave travels to the ground with Alfvén velocity v_A. b_x is rotated -90° by the ionosphere and is observed on the ground as a bipolar change in east-west magnetic field component D. An identical wave is also launched moving south, but is not reflected and cannot be seen in the north.

delay time (half of $t_g = 2.1$ s) to travel from the equator to the receiver in Roberval, so the phase change is seen on the ground 1 s after it occurs. The field line displacement is assumed to take place along a length short compared to the total length of the line. The disturbance is shown in Figure 7 just as it begins. It will shortly separate into two similarly shaped components, one dimple of displacement travelling north and the other south. When both components have moved away from the equator the field line there is assumed to return to its previous position. Each component travels down the field line as a transverse-mode (shear) wave with Alfvén velocity v_A, and is seen on the ground some time after the VLF phase signal.

Associated with the north-moving disturbance is a magnetic field component b_x which lies in the meridional plane and is perpendicular to the undisturbed geomagnetic field B. As stated by *Rietveld et al.* [1978], $b_x = B\,d\xi/ds$, where ξ is the meridional displacement and s is the distance along the field line. Note that for an inward displacement of the duct, associated with a increase in VLF phase ϕ_c, the component b_x is outward on the north half of the disturbance and inward on the south half. Because of the rotation of the hydromagnetic signal caused by the ionosphere, an outward b_x becomes $-D$ on the ground. The bipolar shape of the D versus ϕ_c correlation is due to the bipolar shape of the magnetic field signal b_x as it arrives at the base of the duct. (The south-moving disturbance has the same shaped field, though the negative b_x bump reaches the southern ionosphere first, of course. In Figure 5 there appears to be little if any pulsation echoing; the south-moving wave is not reflected and is not observed in the north.)

The center of the disturbance reaches the ground halfway between the correlation peaks at 18 and 30 s, or 24 s after the phase change is seen. Including the 1-s travel time for the phase effects, the hydromagnetic wave takes a total of 25 s to travel from the equator down the field line to the ground. Using *Park*'s [1972] DE 1 (diffusive equilibrium) plasma density model as above and integrating the Alfvén velocity $v_A = B/(4\pi \times 10^{-7}\rho)^{1/2}$, where ρ is the mass density, we calculate a theoretical travel time of 26 s, in good agreement with the observations. Each transient disturbance has a duration given roughly by the interval between the peaks in the correlation, or about $30 - 18 = 12$ s. Given a one-hop travel time for the pulsation of $2 \times 25 = 50$ s, the average disturbance thus occupies only about one-quarter of the length of the field line.

A likely source for the field-line disturbance is a compressional hydromagnetic wave propagating inward in the equatorial region, probably originating at the magnetopause. The period of the wave (≈ 25 s from the data in Figure 5) would preclude the excitation of a field-line resonant oscillation at the location of the Siple-Roberval duct. This is because the fundamental hydromagnetic wave period of this flux tube is ≈ 100 s for the cold plasma density of 275 cm^{-3} (see *Webb et al.* [1977] for a discussion of a comparison of VLF- and ULF-determined equatorial plasma densities in the magnetosphere). (The compressional wave could have excited a resonant field line at higher latitudes, outside the plasmapause.) The compressional wave, as it propagates past given flux tubes, would cause shear Alfvén waves to propagate down to the northern and southern ionospheres.

Comparison With Other Studies of VLF Phase and Magnetic Pulsations

As mentioned in Section 1, there are two other studies which have compared short-term variations in phase delay and magnetic pulsations, *Andrews* [1977] and *Rietveld et al.* [1978]. *Andrews* [1977] was the first to demonstrate the connection between the two. He presented several examples showing correlations between Pc 5 pulsations and the Doppler shift Δf of whistler mode signals from NLK. Unfortunately, the time resolution of his Doppler data was limited, and he could only resolve oscillations down to periods of 2–3 min. He would have been unable to see transient events such as we have presented or to measure time delays due to HM wave propagation down a field line. Part of the limitation was that his spectrographic receiver was not intended to measure fast changes in Δf and recorded the outputs of its bank of filters on film at a speed of only 1 inch/h (2.5 cm/h). Even so, using a bank of filters to measure Doppler shifts limits the speed of measurement to the filter risetime, and the best Andrews might have achieved would have been a time resolution of 5–10 s. There is no such limitation when using signal phase to measure instantaneous frequency $f = d\phi/dt$. Assuming there is only one signal present, the slope of its phase can be measured with a speed limited only by the signal-to-noise ratio. If desired, we could differentiate the VLF phase signal in Figure 4 and generate a time series of Doppler shifts with a resolution of 1 s or less. On the other hand, the spectrographic receiver or bank-of-filters approach may be necessary when multi-

path propagation occurs, in order to separate whistler mode components on different paths.

Rietveld et al. [1978] reported correlations between Pc 3 pulsations and whistler mode signals from a 6.6-kHz experimental transmitter. There are two main differences between their approach and ours. First, the signals analyzed by *Rietveld et al.* [1978] showed nonlinear amplification (i.e., growth with phase advance) just before the first interval they studied, though not during that interval. Two-tone transmission was not used; its growth-suppression effect had not yet been discovered. Second, the transmission formats, consisting in some cases of pulses, did not allow them to use the relative phase of the signal as such; instead, the instantaneous frequency of the signal was estimated by measuring the slope of the phase-versus-time plot. Thus, the two quantities they studied, Δf and dZ/dt, are essentially the derivatives of the two used above, ϕ_c and either H or D. Their frequency measurements Δf tend to be noisier than our phase measurements ϕ_c, and their measurements do not give a complete coverage in time during their two events. On the other hand, using instantaneous frequency instead of phase and dZ/dt instead of H or D, they were not troubled by the need to filter out long-term signal variations. Except for these differences, both approaches are comparable.

5. CONCLUSIONS

Andrews [1977], *Rietveld et al.* [1978], and this report all support the proposal that hydromagnetic waves affect VLF propagation in whistler mode ducts. The radial magnetic field motions induced by the HM waves change the phase delay of the VLF signals. The observations presented here also provide convincing evidence for the influence of the ionosphere on measurements made on the Earth's surface: the meridional magnetic field motions in the magnetosphere are rotated to become east-west magnetic variations under the ionosphere.

The Siple-Roberval measurements show a time delay between VLF phase changes occuring near the equator and magnetic field changes at the base of the duct consistent with the propagation of a hydromagnetic wave from the equator down the field line to the ground. The correlation between VLF phase and variations in the east-west geomagnetic field component has a bipolar shape, indicating that the length of the average duct displacement event is only a small portion of the total length of the field line. This differs from the standing-wave resonant field-line pulsations reported previously, and may be evidence that coupling between pulsations on field lines at different L values occurs primarily through the equatorial region.

The advantages of the continuous two-tone LICO1 signal combined with phase analysis as used in the Siple-Roberval experiment reported here are several. First, a two-tone signal tends to suppress the temporal VLF wave growth and associated phase shift that can otherwise mask path-related phase changes, and allows phase errors due to multipath fading to be corrected. Second, a continuous transmission allows the phase of the received signal to be measured and used directly. Phase may be a less noisy measure of path conditions than its time derivative, the Doppler shift Δf. The potential quality of the data is shown by the lower panel of Figure 5, which we believe is the first published spectrogram of variations in whistler mode phase delay. When long-term measurements are needed for electric field or plasma flux studies, using phase directly eliminates the errors associated with integrating Δf to find t_p. Third, compared to Navy transmitters such as NLK, the lower frequency of the Siple transmitter allows propagation on higher-latitude paths, and on daytime as well as nighttime paths. Fourth, the time resolution achieved with phase analysis is sufficient to observe delays between changes in the VLF phase path and changes in the magnetic field, and it may be possible to study the shape of transient field-line disturbances.

There are also some disadvantages to this technique. One is the computational workload necessary to extract phase data from an analog field recording. If two-tone phase delay is to be used on a routine basis, it will be desirable to measure it directly at the receiver. A second limitation during multipath propagation is the inability to separate signals on different whistler mode paths. These signals may exhibit different phase behavior. Narrow-band filtering as in *Thomson*'s [1981] method of spectrographic group delays may be necessary, though with an unavoidable decrease in time resolution. Third, we cannot measure the total value of phase delay t_p, but only changes with time (incremental phase delay).

The percentage of time when a two-tone transmission from Siple can be received in usable form in the northern hemisphere is not known and should be the subject of further research. The problem is that signals for phase analysis have been selected mostly to study growth and triggering, which occur in 78% of the data records analyzed to date. Even so, Doppler shifts due to duct motion are briefly seen, when not masked by growth, in 53% of these records. The LICO1 record presented here is the only two-tone signal of this duration that has been examined so far.

Finally, we note that phase analysis of Siple signals might also help to measure plasma flow between the ionosphere and magnetosphere. The errors encountered by *Andrews et al.* [1978] and *Andrews* [1980] in estimating magnetospheric plasma flux over time intervals longer than 90 min were primarily in integrating the Doppler shift Δf to find changes in phase delay t_p. Using relative phase ϕ directly instead of Δf would greatly reduce this error. *Thomson*'s [1981] technique as used by *Saxton and Smith* [1989] measures Doppler shift averaged over a 15-min interval (with an error of ± 0.03 Hz), and integration is not a concern in their case. However, the problem of accurately measuring group delay is common to both. *Andrews'* [1980] reported error in measuring t_g was about ± 1 ms, that of *Saxton and Smith* [1989] was ± 2 ms. For comparison, the error in estimating incremental t_p using phase analysis is roughly 100 times better, perhaps about 0.05 rev at 4 kHz or about 13 μs. Yet, group delay can be determined from a knowledge of phase delay as a function of frequency, since $t_g = t_p + f\, dt_p/df$. This suggests that with an appropriate broad-band signal we might be able to improve the measurement of incremental VLF group delay as well. Perhaps some scheme can be invented that uses phase analysis of, say, frequency ramps spanning a range of 1 kHz (signals available from the Siple transmitter) to measure changes in group delay.

Acknowledgments. The authors thank R. A. Helliwell and D. L. Carpenter for valuable discussions. The phase analysis of LICO1 signals was performed by E. Paschal as part of a Ph.D.

thesis at Stanford University. Stanford work at Siple Station and Roberval was supported by the Division of Polar Programs of the National Science Foundation under grants DPP83-170924, DPP83-185084, and DPP86-13783.

The Editor thanks K. Bullough and K. Takahashi for their assistance in evaluating this paper.

REFERENCES

Andrews, M. K., Magnetic pulsation behaviour in the magnetosphere inferred from whistler mode signals, *Planet. Space Sci., 25,* 957–966, 1977.

Andrews, M. K., Night-time radial plasma drifts and coupling fluxes at $L = 2.3$ from whistler mode measurements, *Planet. Space Sci., 28,* 407–417, 1980.

Andrews, M. K., F. B. Knox, and N. R. Thomson, Magnetospheric electric fields and protonospheric coupling fluxes inferred from simultaneous phase and group path measurements on whistler mode signals, *Planet. Space Sci., 26,* 171–183, 1978.

Andrews, M. K., L. J. Lanzerotti, and C. G. Maclennan, Rotation of hydromagnetic waves between the magnetosphere and the ground, *J. Geophys. Res., 84,* 7267–7270, 1979.

Chang, D. C. D., R. A. Helliwell, and T. F. Bell, Side-band mutual interactions in the magnetosphere, *J. Geophys. Res., 85,* 1703–1712, 1980.

Dowden, R. L., A. D. McKay, L. E. S. Amon, H. C. Koons, and M. H. Dazey, Linear and nonlinear amplification in the magnetosphere during a 6.6 kHz transmission, *J. Geophys. Res., 83,* 169–181, 1978.

Hasegawa, A., and L. J. Lanzerotti, On the orientation of hydromagnetic waves in the magnetosphere, *Rev. Geophys., 16,* 263–266, 1978.

Hughes, W. J., and D. J. Southwood, An illustration of modification of geomagnetic pulsation structure by the ionosphere, *J. Geophys. Res., 81,* 3241–3247, 1976.

Inoue, Y., Wave polarizations of geomagnetic pulsations observed in high latitudes on the earth's surface, *J. Geophys. Res., 78,* 2959–2976, 1973.

Nuttall, A. H., Some windows with very good sidelobe behavior, *IEEE Trans. Acoust. Speech Signal Process., ASSP-29,* 84–91, 1981.

Park, C. G., Whistler observations of the interchange of ionization between the ionosphere and the protonosphere, *J. Geophys. Res., 75,* 4249–4260, 1970.

Park, C. G., Methods of determining electron concentrations in the magnetosphere from nose whistlers, *Tech. Rep. 3454-1,* Radiosci. Lab., Stanford Electron. Labs., Stanford Univ., Stanford, Calif., 1972.

Park, C. G., D. L. Carpenter, and D. B. Wiggin, Electron density in the plasmasphere: Whistler data on solar cycle, annual, and diurnal variations, *J. Geophys. Res., 83,* 3137–3144, 1978.

Paschal, E. W., Phase measurements of very low frequency signals from the magnetosphere, Ph.D. thesis, Stanford University, Calif., 1988.

Paschal, E. W., Whistler precursors on a VLF transmitter signal, *J. Geophys. Res., 95,* 225–231, 1990.

Paschal, E. W., and R. A. Helliwell, Phase measurements of whistler mode signals from the Siple VLF transmitter, *J. Geophys. Res., 89,* 1667–1674, 1984.

Rietveld, M. T., R. L. Dowden, and L. E. S. Amon, Micropulsations observed by whistler mode transmissions, *Nature, 276,* 165–167, 1978.

Saxton, J. M., and A. J. Smith, Quiet time plasmaspheric electric fields and plasmasphere-ionosphere coupling fluxes at $L = 2.5$, *Planet. Space Sci., 37,* 283–293, 1989.

Stassinopoulos, E. G., L. J. Lanzerotti, and T. J. Rosenberg, Temporal variations in the Siple Station conjugate area, *J. Geophys. Res., 89,* 5655–5659, 1984.

Thomson, N. R., Causes of the frequency shift of whistler mode signals, *Planet. Space Sci., 24,* 447–454, 1976*a*.

Thomson, N. R., Electric fields from whistler mode Doppler shifts, *Planet. Space Sci., 24,* 455–458, 1976*b*.

Thomson, N. R., Whistler mode signals: Spectrographic group delays, *J. Geophys. Res., 86,* 4795–4802, 1981.

Webb, D. C., L. J. Lanzerotti, and C. G. Park, A comparison of ULF and VLF measurements of magnetospheric cold plasma densities, *J. Geophys. Res., 82,* 5063–5072, 1977.

L. J. Lanzerotti and C. G. Maclennan, AT&T Bell Laboratories, 600 Mountain Avenue, Murray Hill, NJ 07974

E. W. Paschal, STAR Laboratory, 324 Durand Building, Stanford University, Stanford, CA 94305.

(Received December 13, 1988;
revised November 22, 1989;
accepted December 21, 1989.)